Progress In Electromagnetics Research C, Vol. 57, 61–69, 2015

A New Class of Compact Linear Printed Antennas

Mohammad Almalkawi[1, *], Khair Alshamaileh[1], Said Abushamleh[2], and Hussain Al-Rizzo[2]

Abstract—A new miniaturization methodology suitable for printed linear antennas is presented. Miniaturization is accomplished by replacing a linear radiator element of a conventional antenna with a compact continuously varying-impedance profile governed by a truncated Fourier series. A design example of a printed half-wavelength dipole antenna is designed and realized in microstrip technology. The performance of the proposed antenna is compared with its equivalent uniform dipole to highlight the performance equivalency. With a 25% reduction in the dipole arm length, both antennas show a measured peak gain and a fractional bandwidth of 5.4 dBi and 16%, respectively at 2.5 GHz; hence, the overall electrical performance is preserved. It will be shown that the design procedure is systematic and accurate. The proposed approach has potential for achieving advanced frequency characteristics, such as broad- and multi-band antenna responses.

1. INTRODUCTION

With the advent of modern wireless technologies and an ever-growing dependence of our daily life on mobile communication platforms, compact low-cost antennas have gained considerable attention [1–15]. Contemporary handheld transceivers, printed phased-array systems, and passive radio-frequency identifications (RFIDs) have imposed stringent requirements on antenna physical sizes, especially those operating at low frequencies. As a result, the subject of antenna miniaturization continues to receive serious research interest. Traditionally, printed antenna miniaturization techniques have relied on shortening the length of linear antenna radiators at the expense of the radiators' width and/or height. This have been demonstrated through several concepts, including high permittivity loading materials and elements [1–3], photonic band-gap structures [4, 5], inverted-F configurations [6, 7], folding an antenna radiator into a single- or a multi-layer structure [8–10], slots on antenna radiator elements [11, 12], fractal geometries [13], and bio-inspired optimization methods to minimize an antenna topology [14, 15]. To some extent, miniaturization of printed antennas using loading materials causes the quality factor to increase and therefore decreases the bandwidth, radiation efficiency, and may influence the level of polarization purity [16, 17]. Moreover, multi-layer structures add to the manufacturing cost and may not be an option for a given design (e.g., available volume constraint). Low radiation resistance due to small aperture area is another challenge in utilizing multi-layer configurations. Alternatively, size reduction through modifying and optimizing antenna geometries (e.g., inverted-F, fractal, meander lines, adding slots, etc.) is more preferable. Such geometries, however, may introduce high current concentrations, and consequently increase ohmic losses or, equivalently, decrease the gain. While thick linear antennas are considered broadband and thin radiator elements are narrowband, increasing the flare angle of a bow-tie antenna results in increasing the bandwidth with a total antenna length slightly less than a half-wavelength. The associated length reduction, however, is not comparable with those achieved using for example, fractal and meander line geometries.

Received 21 March 2015, Accepted 15 April 2015, Scheduled 21 April 2015

* Corresponding author: Mohammad Almalkawi (Mohammad.Almalkawi@rockets.utoledo.edu).

[1] Electrical Engineering and Computer Science (EECS) Department, the University of Toledo, Toledo, Ohio 43606, USA.

[2] Department of Systems Engineering, University of Arkansas at Little Rock, Little Rock, Arkansas 72204, USA.

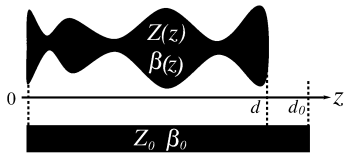

Figure 1. A uniform transmission line and its miniaturized profile following a Fourier series profile along the propagation axis Z.

It is therefore desirable to explore new antenna miniaturization methods that do not result in significant degradation of the antenna performance in terms of gain, radiation pattern, radiation efficiency, and bandwidth. To this end, we propose a new antenna miniaturization method inspired by the general theory used to design compact non-uniform transmission line (NTL) transformers. This analogy can be established by modulating the impedance profile of resonant antenna radiators following Fourier series (Fig. 1) in order to obtain compact antenna radiators without incorporating additional reactive loading elements and/or materials. In this context, an antenna radiator is considered as a two-port network and the effective permittivity of the surrounding medium is evaluated experimentally. The proposed methodology offers several advantages over existing techniques:

- First, it uses accurate and systematic design procedure to work forward from a specification to a final prototype.
- Second, the flexibility in controlling the antenna physical dimensions as part of the optimization process allows straightforward fabrication.
- Third, the approach can be easily applied to a variety of planar single and array antennas including frequency-dependent and -independent antennas.
- Finally, an important property of the Fourier based variable impedance function used in this work is that the resulting shape of the antenna radiator does not comprise sharp discontinuities, thus minimal influence on the antenna overall performance including bandwidth, radiation pattern, and efficiency.

In Section 2, the step-by-step procedure of the proposed Fourier based miniaturization concept and their pertinent equations is discussed. Section 3 presents a design example of a printed dipole antenna fed by balanced microstrip line. Section 4 reports the experimental results, while outcomes of this work are summarized in Section 5.

2. MINIATURIZATION METHOD

The theory pertaining to the design of a compact antenna radiator element exhibiting variable impedance profile is demonstrated in this section. Fig. 1 illustrates a typical uniform transmission line (UTL) with a length, characteristic impedance and propagation constant of d_0, Z_0 and $\beta 0$, respectively, versus an equivalent NTL of length d, varying characteristic impedance $Z(z)$, and propagation constant $\beta(z)$. Referring to Fig. 1, the synthesis of an NTL starts by evaluating the $A_0B_0C_0D_0$ matrix [18] of a UTL defined by

$$\begin{bmatrix} A_0 & B_0 \\ C_0 & D_0 \end{bmatrix} = \begin{bmatrix} \cos(\theta_o) & jZ_0\sin(\theta_o) \\ jZ_0^{-1}\sin(\theta_o) & \cos(\theta_o) \end{bmatrix} \tag{1}$$

where $\theta_0 = \beta_0 d_0$ is the electrical length of the UTL. The NTL is designed so that its $ABCD$ parameters at a given frequency, f, are equal to those of the UTL. Moreover, compactness is achieved by choosing the length d to be smaller than d_0. It was observed that d can be reduced up to approximately two-thirds of d_0 in order to maintain a reasonable aspect ratio between a line length and a maximum resultant width produced by the underling design method. This is to ensure that the excitation wave propagates along the line longitudinal direction. Next, the non-uniform line is subdivided into K electrically commensurate short sections, each with a length of Δz as given in (2),

$$\Delta z = \frac{d}{k} \ll \lambda_g = \frac{c}{\sqrt{\varepsilon_{eff}}f} \tag{2}$$

where c is the speed of light in vacuum and λ_g the guided wavelength. The total $ABCD$ matrix of the NTL is obtained by multiplying the $ABCD$ parameters of each individual section as follows [18]

$$\begin{bmatrix} A & B \\ C & D \end{bmatrix}_{Z(z)} = \begin{bmatrix} A_1 & B_1 \\ C_1 & D_1 \end{bmatrix} \cdots \begin{bmatrix} A_i & B_i \\ C_i & D_i \end{bmatrix} \cdots \begin{bmatrix} A_K & B_K \\ C_K & D_K \end{bmatrix} \tag{3}$$

where the $ABCD$ parameters of the ith segment are

$$A_i = D_i = \cos(\Delta\theta) \tag{4a}$$

$$B_i = Z^2 \left((i-0.5)\,\Delta z\right) C_i = jZ \left((i-0.5)\,\Delta z\right) \sin\left(\Delta\theta\right) \quad i = 1, 2, \ldots K \tag{4b}$$

$$\Delta\theta = \frac{2\pi}{\lambda}\Delta z = \frac{2\pi}{c} f \sqrt{\varepsilon_{eff}}\,\Delta z \tag{4c}$$

The design of a non-uniform antenna radiator is considered as a symmetrical pair of separated strip conductors (e.g., dipoles), or a single strip and a ground plane (e.g., monopoles), on a dielectric material. Hence, the effective dielectric constant in (4c), ε_{eff}, for the medium surrounding each segment has no explicit formula. Therefore, ε_{eff} can be determined experimentally as in [19] by noting the resonant frequencies f_0 and f_d of a given antenna radiator length in air and the dielectric material, respectively, using

$$\varepsilon_{eff} = \frac{f_0^2}{f_d^2}. \tag{5}$$

Then, the normalized characteristic impedance of each section [20] can be calculated through the following truncated Fourier series expansion

$$\ln\left(\bar{Z}(z)\right) = \sum_{n=0}^{N} C_n \cos\left(\frac{2\pi n z}{d}\right) \tag{6a}$$

$$\bar{Z}(z) = \frac{Z(z)}{Z_o} \tag{6b}$$

where C_n's (n = 1, 2, ..., N) are the Fourier coefficients. N is the number of coefficients and Z_0 the characteristic impedance of the line. It is worth mentioning that symmetric or asymmetric line profiles are attainable by excluding or including the Fourier series orthogonal sine terms, respectively.

The $ABCD$ matrix of the compact NTL can now be found by having its parameters as close as possible to the $A_0B_0C_0D_0$ parameters of the desired UTL at a specific design frequency. Instead of optimizing 'K' 2×2 $ABCD$ matrices to minimize (7), we chose the Fourier series coefficients in (6a) as the optimization variables. Hence, search space is reduced, as such coefficients are bounded between [−1, 1]. Finding the optimum values of the Fourier coefficients (C_n's) can be acquired through minimizing the following mean squared error function which has been selected as a measure to guide the optimization process,

$$Error = \sqrt{\frac{1}{4}\left(|A-A_0|^2 + Z_0^{-2}\,|B-B_0|^2 + Z_0^2\,|C-C_0|^2 + |D-D_0|^2\right)}. \tag{7}$$

The error function in (7) should be accompanied with constraints on physical dimensions as expressed in (8) to avoid restrictions (e.g., minimum line width) imposed by standard PCB manufacturing methods

$$\bar{Z}_{\min} \le \bar{Z}\,(z) \le \bar{Z}_{\max} \tag{8a}$$

$$\bar{Z}\,(0) = \bar{Z}\,(d) = 1 \tag{8b}$$

where $\bar{Z}_{\min}$ and $\bar{Z}_{\max}$ are the minimum and maximum normalized impedances corresponding to the maximum and minimum line widths, respectively. To solve the above bound-constrained non-linear optimization problem, a trust-region-reflective algorithm which has strong convergence properties [21] is adopted using MATLAB. In this iterative optimization process, there is no unique solution for the unknown Fourier coefficient values; and each iteration results in a different set. However, the optimal response accompanied with an impedance profile that is realizable and complies with (8a) and (8b) is considered in the subsequent design steps (e.g., fine optimization and verification in a full-wave

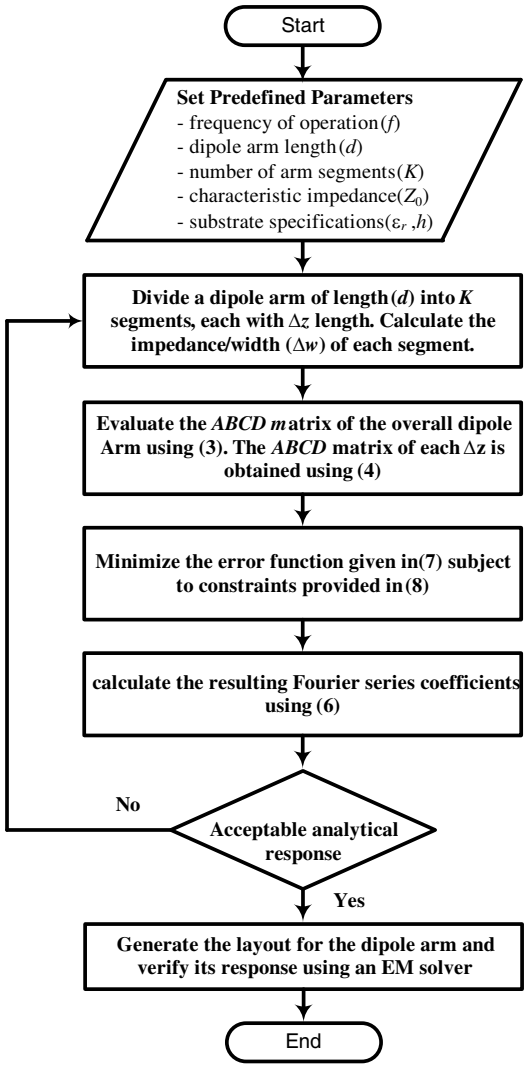

Figure 2. Flowchart demonstrating the general design/optimization procedure of a compact non-uniform dipole arms.

simulator to account for parasitics and detailed layouts). Fig. 2 shows a flowchart summarizing the design procedure.

It is worth pointing out that the proposed methodology is valid in case of designing an antenna array that is made of symmetrical pairs of conductive strip radiators (e.g., Yagi-Uda or log periodic dipole array); where each pair can be independently designed and then assembled to construct a compact array. This simplifies further the realization of complex and compact antenna structures, while significantly reducing uncertainties in the design phase. Considering that a single dipole radiator can be used as a unit cell for a variety of linear antenna arrays, a planar dipole antenna was selected as a design example under this work.

3. REDUCED LENGTH DIPOLE ANTENNA

Uniform and compact non-uniform half-wavelength microstrip-fed dipole antennas comprising symmetrical arms are designed to operate at 2.5 GHz. Considering Rogers RO4835 substrate with thickness of 1.524 mm, dielectric constant of 3.66, loss tangent of 0.0037, and copper cladding of 17 µm, the $A_0B_0C_0D_0$ parameters of a conventional uniform dipole arm of one-quarter wavelength long at

the design frequency are calculated. These parameters are used as reference values for the subsequent optimization process that follow the design procedure demonstrated in Section 2. Equation (5) yields a value of ε_{eff} equals to 1.5, and the $ABCD$ relations in (4) hold for the non-uniform arm. Upon achieving an error value of 3×10^{-8} from minimizing (7), the generated Fourier coefficients, given in Table 1, are collected and reincorporated in (6) with number of coefficients, N equals to 10 sufficient to obtain the desired electrical and physical properties of the non-uniform dipole arm.

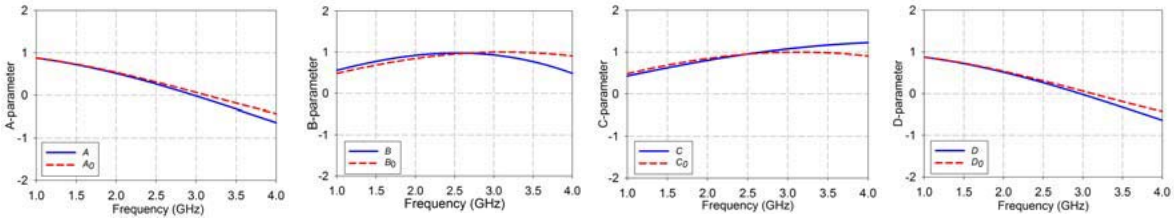

Figure 3. Optimized $ABCD$ parameters of the proposed non-uniform dipole arm compared to the conventional $A_0B_0C_0D_0$ parameters of the uniform arm.

Table 1. Optimized Fourier coefficients for the compact dipole arm.

C_0	C_1	C_2	C_3	C_4	C_5
0.1271	0.8843	−0.1898	−0.2984	0.1487	0.0563
C_6	C_7	C_8	C_9	C_{10}	–
−0.3969	−0.3958	−0.0566	0.1281	−0.0071	

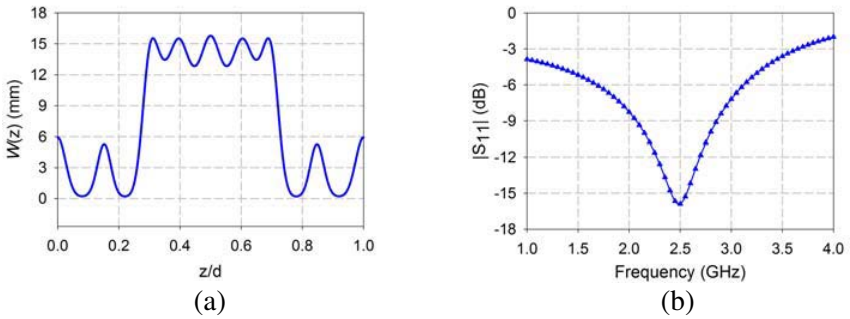

Figure 4. (a) The resulting width profile of the optimized non-uniform dipole arm; and (b) its analytical S-parameter reflection coefficient response.

Figure 3 illustrates a comparison between the converged $ABCD$ parameters of both uniform and non-uniform arms. Although the equivalency is enforced at 2.5 GHz, the optimized non-uniform dipole arm is equivalent to the uniform one within the design bandwidth (i.e., 2.3–2.7 GHz). The resultant non-uniform arm has a width varying between 0.2 and 15.6 mm and a resonant frequency (f_c) of 2.5 GHz. Here, width variations correspond to the optimized Fourier coefficients, while the desired input port impedance is maintained unaltered as stated in (8b).

Figure 4(a) depicts the total width variation, $W(z)$, versus the normalized line length, and a fixed periodic segmentation ($\Delta z/d$) of the non-uniform impedance profile, while Fig. 4(b) shows its input port matching, $|S_{11}|$, calculated using (9) with a characteristic impedance (Z_o) of 50-Ω.

$$S_{11} = \frac{A + B/Z_o - CZ_o - D}{A + B/Z_o + CZ_o + D} \tag{9}$$

4. EXPERIMENTAL RESULTS

Upon the successful implementation of the compact dipole arm, non-uniform and conventional uniform microstrip-fed dipole antennas with 50-Ω input terminal were constructed. Fig. 5(a) shows the structure of the uniform printed dipole antenna, while Fig. 5(b) demonstrates its miniaturized topology comprising two non-uniform arms. With the aid of *ANSYS-HFSS* [22], full-wave electromagnetic simulations were carried out to evaluate the performance of the configurations in Fig. 5.

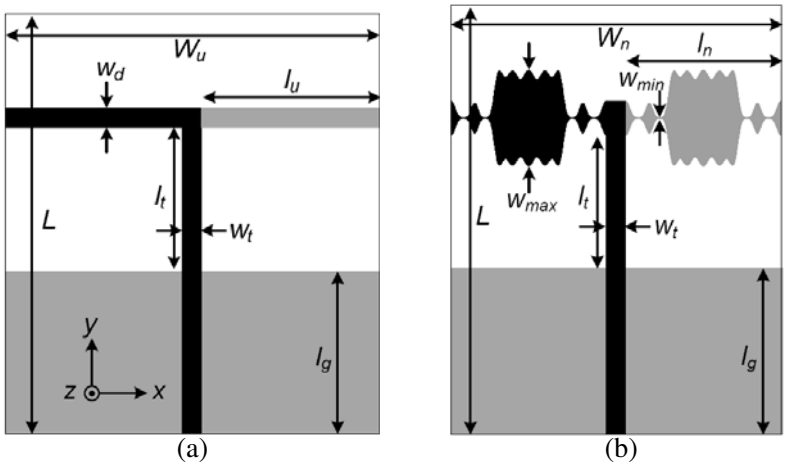

Figure 5. Illustrative configurations of: (a) conventional microstrip dipole antenna with uniform radiators; and (b) proposed dipole antenna with miniaturized arms exhibiting Fourier based profiles. Black and gray color strips refer to upper and lower dipole planes, respectively.

The optimal values (in mm) of each geometric parameter were found to be: $L = 55$; $W_u = 60$; $W_n = 50$; $l_g = 22$; $l_t = 20.9$; $w_t = 2.9$; $l_u = 21.3$; $l_n = 15.9$; $w_d = 2$; $w_{\max} = 9.5$; $w_{\min} = 0.2$. To verify the performance experimentally, designs of Fig. 5 were fabricated and tested using SMA connectors mounted at the end of the feed-line and the edge of the ground plane.

Figure 6 depicts the measured reflection coefficient, $|S_{11}|$ results for the reference and the proposed antennas. Both measurements exhibit similar trends with center frequency of 2.5 GHz and return loss > 14 dB. Furthermore, 16% fractional bandwidth is preserved for both designs.

The resulting radiation efficiency of the uniform and compact non-uniform antennas is shown in Fig. 7. The estimated efficiencies are in good agreement and higher than 96% over the operating bandwidth. This indicates that both antennas are exposed to approximately the same loss factors (i.e., ground, conductor, and dielectric losses).

Figure 8 illustrates the measured far-field radiation patterns for both conventional and proposed antennas at 2.5 GHz. The experiments were performed in anechoic chamber with the antenna mounted on an electronically controlled turntable. Scrutiny of Fig. 8 shows that the radiation patterns of both antennas exhibit consistent behavior and demonstrates low cross-polarization levels (< -15 dB) in all three cutting planes. Both antennas result in a peak gain of 5.4 dBi at 2.5 GHz, measured at the antenna directivity direction which coincides with the y axis direction as shown in Fig. 5(a).

It is worth mentioning that the proposed non-uniform arm has no degradation on the overall electrical performance by virtue of the slow impedance transitions resulting from use of Fourier coefficients. Given that both antennas in Fig. 5 are designed for the same center frequency and fractional bandwidth, a 25% length reduction on the dipole arm length is obtained.

The simulated surface current of the proposed antenna radiator is shown in Fig. 9. The surface current concentrated mainly on the narrow segments and edges of the non-uniform dipole arms where the conversion of surface waves into free-space waves takes place [23]. Although the antenna arms are shortened, the operating frequency is maintained by increasing the path length of the antenna surface current that compensates the achievable length reduction.

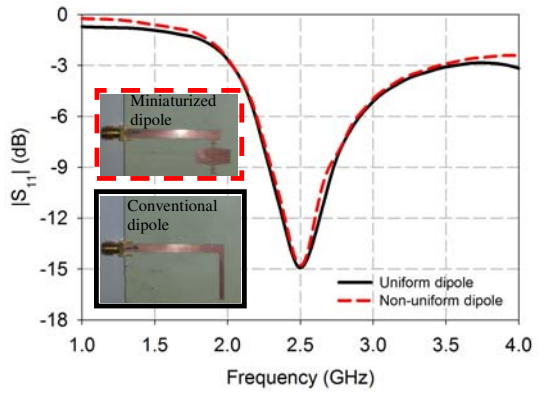

Figure 6. Measured return loss of the conventional and proposed dipole antennas.

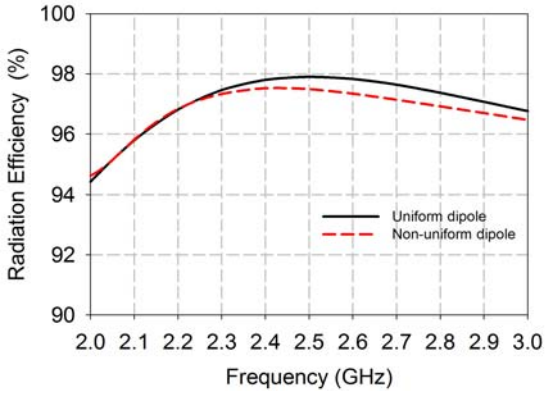

Figure 7. Evaluated antenna efficiency of the conventional and proposed dipole antennas.

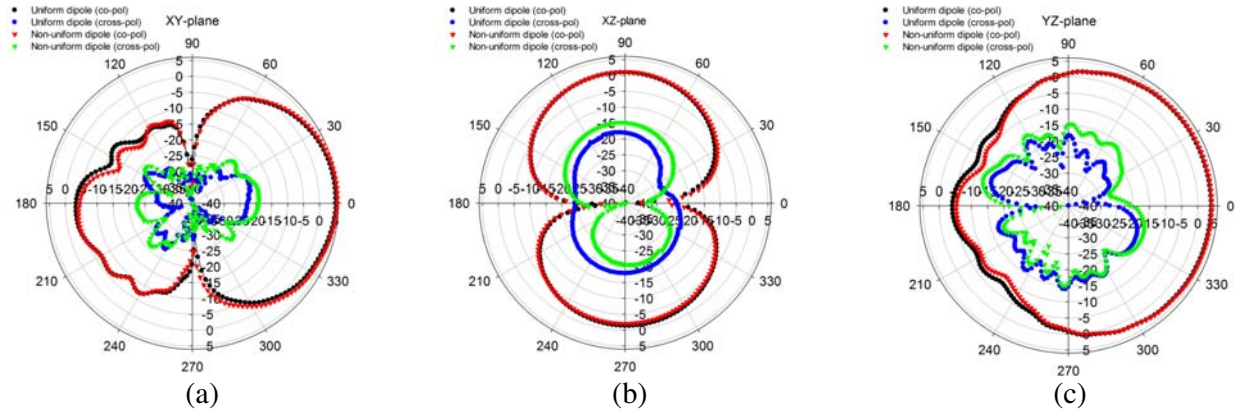

Figure 8. Measured far-field radiation patterns of perturbed and uniform impedance microstrip dipole antennas at 2.5 GHz: (a) XY-plane; (b) XZ-plane; and (c) YZ-plane.

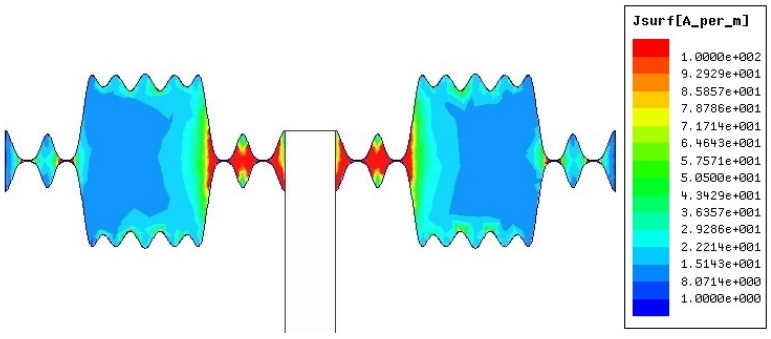

Figure 9. Simulated current distribution of the antenna's non-uniform arms at 2.5 GHz.

In general, the experimental results are in good agreement with the theoretical predictions, and this illustrates the fidelity of the proposed miniaturization approach. Depending on how the impedance profile is modulated, the proposed approach has further advantages in realizing compact radiator elements possessing advanced frequency characteristics such as multi-band resonances and broad impedance matching.

5. CONCLUSION

In this paper, a systematic transmission line oriented approach to the miniaturization of printed linear antennas was proposed. Length reduction of an antenna radiator element is accomplished by replacing the uniform radiators by their analogous reduced-length elements exhibiting continuous impedance perturbation. The impedance modulation of the radiator profile follows a truncated Fourier series whose width variations correspond to the optimized Fourier coefficients, while an element input impedance is maintained unaltered. A fabricated proof-of-concept microstrip dipole antenna has validated the underlying principle. In comparison with the uniform dipole arm length, a 25% length reduction was achieved without degradation in the operating bandwidth, gain level, radiation pattern, and efficiency.

Furthermore, the proposed methodology circumvents issues that may exist in other antenna miniaturization techniques where sharp discontinuities, loading elements, and multi-layer structures are employed.

REFERENCES

1. Colburn, J. and Y. Rahmat-Samii, "Patch antennas on externally perforated high dielectric constant substrates," *IEEE Trans. on Antennas Propag.*, Vol. 47, No. 12, 1785–1794, Dec. 1999.
2. Byungje, L. and F. J. Harackiewicz, "Miniature microstrip antenna with a partially filled high-permittivity substrate," *IEEE Trans. on Antennas and Propag.*, Vol. 50, No. 8, 1160–1162, Aug. 2002.
3. Antoniades, M. and G. Eleftheriades, "Multiband compact printed dipole antennas using NRI-TL metamaterial loading," *IEEE Trans. on Antennas and Propag.*, Vol. 60, No. 12, 5613–5626, Dec. 2012.
4. Sigalas, M. M., R. Biswas, and K.-M. Ho, "Theoretical study of dipole antennas on photonic band-gap materials," *Microw. Opt. Technol. Lett.*, Vol. 13, No. 4, 205–209, 1996.
5. Eldek, A., "A miniaturized patch antenna at 2.4 GHz using uni-planar compact photonic band gap structure," *Microw. Opt. Technol. Lett.*, Vol. 50, No. 5, 1360–1363, 2008.
6. Azad, M. and M. Ali, "A new class of miniature embedded inverted-F antennas (IFAs) for 2.4 GHz WLAN application," *IEEE Trans. Antennas Propag.*, Vol. 54, No. 9, 2585–2592, Sept. 2006.
7. Bayraktar, Z., M. Komurcu, Z. Jiang, D. Werner, and P. Werner, "Stub-loaded inverted-F antenna synthesis via wind driven optimization," *IEEE Int. Symposium on Antennas and Propag.*, 2920–2923, Spokane, Washington, Jul. 2011.
8. Chair, R., K. M. Luk, and K.-F. Lee, "Miniature multilayer shorted patch antenna," *Electronics Lett.*, Vol. 36, No. 1, 3–4, Jan. 2000.
9. Zhang, Y. and H.-Y. Yang, "Miniaturized printed folded dipole antennas," *IEEE Antennas and Propag. Society International Symposium*, 1–4, Jun. 2009.
10. Kim, J., M. Nagatoshi, and H. Morishita, "Study on miniaturization of a strip folded dipole antenna with two linear conductors," *Proc. the 5th European Conference on Antennas and Propag.*, 342–345, Rome, Italy, Apr. 2011.
11. Boone, J., S. Krishnan, E. Stefanakos, Y. Goswami, and S. Bhansali, "Coplanar-waveguide-fed folded dipole slot antenna for wireless local area network applications and V-band frequency operations," *IET Microw., Antennas & Propag.*, Vol. 6, No. 5, 583–587, Apr. 2012.
12. Chang, M.-C. and W.-C. Weng, "A dual-band printed dipole slot antenna for 2.4/5.2 GHz WLAN applications," *IEEE Int. Symposium on Antennas and Propag.*, 274–277, Spokane, Washington, Jul. 2011.
13. Oraizi, H. and S. Hedayati, "Miniaturization of microstrip antennas by the novel application of the Giuseppe Peano fractal geometries," *IEEE Trans. Antennas Propag.*, Vol. 60, No. 8, 3559–3567, Aug. 2012.
14. Herscovici, N., M. Osorio, and C. Peixeiro, "Miniaturization of rectangular microstrip patches using genetic algorithms," *IEEE Antennas Wireless Propag. Lett.*, Vol. 1, No. 1, 94–97, 2002.
15. Rengarajan, S. R. and Y. Rahmat-Samii, "On the cross-polarization characteristics of crooked wire

antennas designed by genetic algorithms," *IEEE Int. Symp. on Antennas and Propagation Society*, Vol. 1, 706–709, 2002.

16. Skrivervik, A.K., J.-F. Zürcher, O. Staub, and J. R. Mosig, "PCS antenna design: the challenge of miniaturization," *IEEE Antennas Propag. Mag.*, Vol. 43, No. 4, 12–27, Aug. 2001.
17. Bancroft, R., "Fundamental dimension limits of antennas ensuring proper antenna dimensions in mobile device designs," *Centurion Wireless Technologies*, Westminster, CO.
18. Pozar, D. M., *Microwave Engineering*, 4th Edition, John Wiley & Sons, Inc., Hoboken, NJ, 2011.
19. Campbell, C. K., I. Traboulay, M. S. Suthers, and H. Kneve, "Design of a stripline log-periodic dipole antenna," *IEEE Trans. Antennas Propag.*, Vol. 25, No. 5, 718–721, Sept. 1977.
20. Khalaj-Amirhosseini, M., "Nonuniform transmission lines as compact uniform transmission lines," *Prog. In Electromagnetics Research C*, Vol. 4, 205–211, 2008.
21. Li, Y., "Centering, trust region, reflective techniques for nonlinear minimization subject to bounds," Technical Report 93-1385, Cornell University, NY, USA, Sept. 1993.
22. ANSYS-High Frequency Structure Simulator (HFSS), Ansys, Inc., Canonsburg, PA, 2011.
23. Caratelli, D., R. Cicchetti, G. Bit-Babik, and A. Faraone, "Circuit model and near-field behavior of a novel patch antenna for WWLAN applications," *Microwave and Optical Technology Letters*, Vol. 49, No. 1, 97–100, Jan. 2007.